Numerical Simulation INGAP/GAAS Solar Cell with Hetero Tunnel Junction using A Thin Carbon Nano Tube Layer and Multi Quantum Well

Bita Farhadi[a], Saba Ebrahimpanah[b], Rozita Farhadi[a, *], Younes Sohrabi[c]，Tahereh Abasi[a]

[a]Young Researchers and Elite Club, Kermanshah Branch, Islamic Azad University, Kermanshah ,Iran
[b]Electrical Engineering Department, Faculty of Engineering, Razi University, Tagh-E-Bostan, Kermanshah 67149, Iran
[c]Research Center for Environmental Determinants of Health, Kermanshah University of Medical Sciences, Kermanshah, Iran

Abstract:- **The structure and performance parameters of Double Junction InGaP/GaAs Solar Cell were studied and optimized using Silvaco software and numerically simulated to obtain the maximum possible value of efficiency. Here, we investigated InGaP/GaAs solar cell using a thin Carbon Nanotubes with hetero tunnel junction is modified by adding Multi Quantum Well. It predicted that by combining two different GaAs and CuGaSe Material as quantum well between the layers of the cell, the efficiency would be modified and would increase from % to 49.71%. At last, we compared the performance of solar cells with and without quantum well.**

Keywords: Efficiency, Solar Cells, Double Junction structure, hetero tunnel junction, quantum well, Carbon Nanotube.

1. INTRODUCTION

A solar cell, or photovoltaic cell, a denotation which nowadays has a different meaning, is optimized and effective value of efficiency and it is due to that Multi junction solar cells are solar cells with multiple p-n junctions made of different semiconductor materials, each material's p-n junction will produce electric current in response to various optical radius. The use of multiple semiconductor materials help to absorb extra range of optical radius and improving the solar cells's
*Corresponding author,
E-mail address: rose66f@gmail.com (Rozita Farhadi).
absorbing sunlight to produce efficient electrical energy and best solar cells are now multi-junction and have achieved efficiencies of over 30 percent. The primary sources of energetic particles of concern are protons and electrons trapped in the Van Allen belts, heavy ions trapped in the magnetosphere, cosmic ray protons, and heavy ions, and protons and heavy ions from solar flares [2]. Michalopoulous utilized the tools available from the Silvaco ATLAS device simulator to model the operation of multi-junction solar cells. His work helped prove that ATLAS can use as a useful, efficient tool to help save time and cost to design solar cells. The III-V semiconductors play an important role in solar cell technology, and so far, the III-V semiconductors based solar cells are the commercial cells with the highest efficiency. The most critical parameter of a solar cell is its efficiency, which is quite low for single-junction solar cells. The energy conversion efficiency increased in multi-junction cells, with the reported efficiency of more than 40% [4]. Double junction (DJ) solar cells composed of two subcells, namely, InGaP (top cell, bandgap energy Eg = 1.9eV), GaAs (bottom cell, Eg = 1.42eV) are efficient solar cells which achieved conversion efficiencies of close to 40% and employed in many applications [3-5].

In 2014, a GaInP/GaAs double junction solar cell using the computational numerical modeling TCAD tool Silvaco ATLAS simulated by P. P. Nayak et al. [6], where, Jsc, Voc, and Fill factor found to be 17.33 mA/cm2, 2.66V, and 88.67% respectively. The simulation was done under AM1.5G illumination, exhibiting a maximum conversion efficiency of 34.52% (1 sun) and 39.15% (1000 suns) [7]. A 'quantum well' is a potential well with only discrete energy values . The primary model that used to demonstrate a quantum well is to confine particles, At the beginning there were moved freely in two and three dimensions. A defining property of superlattices is that barriers between wells are so thin for adjacent wells to couples. The structures that made of repeated quantum wells that have barriers those are too thick for adjacent optical radius functions as couples,they called multiple quantum well structures . In solar cells, the quantum wells making up a part of the thin i layer in a p-i-n junction confines the electrons to two dimensions. It means electrons and holes are quantized, having discrete levels of energy. Within the i layer of the junction, the potential energy of an electron is less than the outside layer, so the flow of charge is confined to certain well-defined regions that can be exploited in solar photovoltaics. Quantum wells are grown by molecular beam epitaxy, where atoms of the materials are delivered to crystals using a molecular beam or through chemical vapor deposition, using a flowing gas [9-11].

In this article, the performances of the proposed double junction InGaP/GaAs solar cell using CNT and hetero tunnel junction are modified by adding multi-quantum well between pn junction layers, and the characteristics are numerically simulated, using the two-dimensional device simulator Silvaco Atlas. Moreover, the performances of the cell before and after the addition of the multi-quantum well compared. This paper includes the following sections: In the next section, the modified double junction InGaP/GaAs using CNT and hetero tunnel junction solar cell and the numerical simulation employed here, are presented. A brief description

of the simulation parameters given in Section 3. The results of the simulation presented and discussed in Section 4. Finally, the conclusion is shown in the last section.

2. MODIFIED DOUBLE JUNCTION INGAP/GAAS SOLAR CELL WITH HETERO TUNNEL JUNCTION USING CNT AND NUMERICAL SIMULATION

In this work, the basic structure of the modified Double Junction InGaP/GaAs Solar Cell with hetero tunnel junction using CNT is shown in Fig. 1. This structure from bottom to top include a 200 nm n-GaAs as substrate layer ($n=1\times10^{18}$ cm^{-3}), the 1.390µm n-InAlGaP as BSF layer ($n=5\times10^{18}$ cm^{-3}), the 2.929 µm n-GaAs as Base Layer ($n=2\times10^{17}$ cm^{-3}), the 2 nm CuGaSe as Quantum Well, the 484 nm p-GaAs as Emitter layer ($p=2\times10^{18}$ cm^{-3}), the 40nm p-InGaP as window layer ($p=3\times10^{18}$ cm^{-3}), the 16 nm p-GaAs as tunnel junction ($p=3\times10^{19}$ cm^{-3}), the 15 nm n-InGaP as tunnel junction ($n=5\times10^{19}$ cm^{-3}), the 35 nm n-InAlGaP as BSF Layer ($n=2\times10^{18}$ cm^{-3}), the 55 nm n-InAlGaP as BSF Layer ($n=2\times10^{17}$ cm^{-3}), the 548 nm n-InGaP as Base Layer ($n=7\times10^{15}$ cm^{-3}), the 2 nm GaAs as Quantum Well, the 60 nm p-InGaP as Emitter Layer ($p=2\times10^{18}$ cm^{-3}), the 14 nm p-InAlGaP as window ($p=2\times10^{18}$ cm^{-3}) and the 100 nm CNT.

Anode			
ARC	CNT	100 nm	
Window	InAlGaP	14 nm	p=2$\times10^{18}$ cm^{-3}
Emitter	InGaP	60 nm	p=2$\times10^{18}$ cm^{-3}
Quantum well	GaAs	2 nm	
Base	InGaP	548 nm	n=7$\times10^{15}$ cm^{-3}
BSF	InAlGaP	55 nm	n=2$\times10^{17}$ cm^{-3}
BSF	InAlGaP	35 nm	n=2$\times10^{18}$ cm^{-3}
TJ	InGaP	15 nm	n=5$\times10^{19}$ cm^{-3}
TJ	GaAs	16 nm	p=3$\times10^{19}$ cm^{-3}
Window	InGaP	40 nm	p=3$\times10^{18}$ cm^{-3}
Emitter	GaAs	484 nm	p=2$\times10^{18}$ cm^{-3}
Quantum well	CuGaSe	2 nm	
Base	GaAs	2.929 µm	n=2$\times10^{17}$ cm^{-3}
BSF	InAlGaP	1.39 µm	n=5$\times10^{18}$ cm^{-3}
BSF	GaAs	200 nm	n=1$\times10^{18}$ cm^{-3}
Cathode			

Fig.1. InGaP/GaAs Solar cell modified by multi-quantum well.

Every solid has its individual particles of a substance are in fixed position with respect to each other because there is not enough thermal energy to overcome the intermolecular interactions between the particles . A solid substance that has a activity between of an insulator and most of metals, either due to the addition of an impurity or because of temperature effects. Devices made of semiconductors, particulary made of silicon ,yhose are essential components of electronic ciruits. Semiconductors are classified by the fully occupied valence band and unoccupied conduction band with small band gap that placed between these two bands, it takes a certain amount of energy to excite the electrons from the valence to conduction band. several bands of energy and forbidden from other regions. The term "bandgap" refers to the energy difference between the top of the valence band and the bottom of the conduction band. However, for an electron to jump from a valence band to a conduction band, a specific minimum amount of energy for the transition is required.

In multi-junction structures, different levels are used to absorb the most significant possible part of the sunlight passing the semiconductor and convert it to electrical energy. In a single solar cell, efficiency is quite limited. It happens because the semiconductor cannot absorb the entire spectrum of the solar radiation impinging on it. That is, photons with energy less than the bandgap energy of the semiconductor are lost in the passage through the semiconductor without interacting with it, or bumping into the crystal lattice, converting part of their energy to heat. In any case, they are not involved in converting solar energy into electrical energy, and this happens because they do not have sufficient energy to excite electrons from the valence band into the conduction band. Moreover, in photons with energy higher than the bandgap energy, the extra energy is lost. Since a part of the energy required exciting an electron from the valence band to the conduction band, creating one electron-hole pair is absorbed, the excess photon energy is converted into heat. Figure 2 showing the range of bandgap and influence on spectrum irradiance.
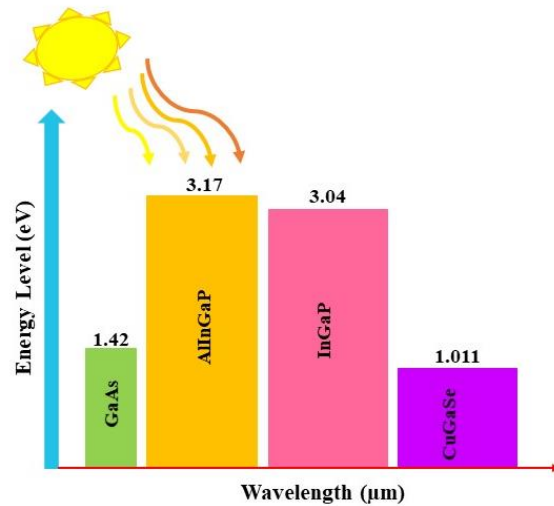
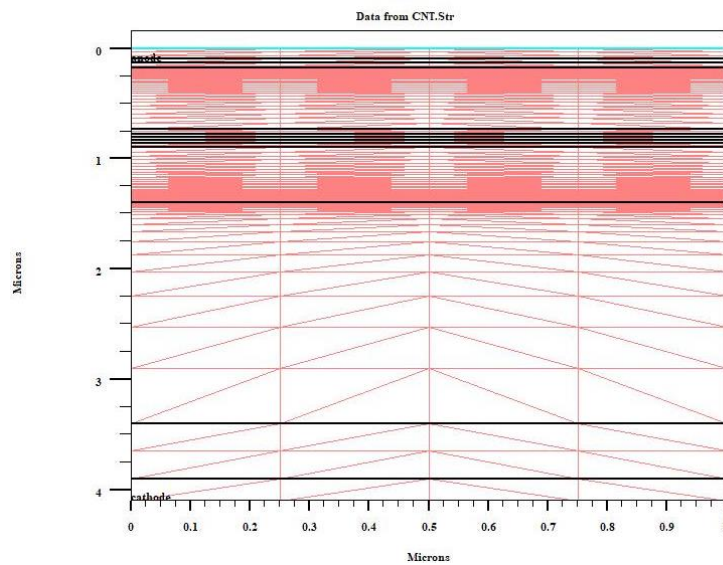Fig.2. Solar spectrum and response of semiconductors with different bandgaps.

Fig.3. The mesh structure of the model.

3. SIMULATION PARAMETERS

The proposed model is simulated using the 2D Atlas TCAD toll and requires the material parameters related to each layer and material in the cell structure as input parameters. The material parameters properties used in the simulation are given in Table.1. The meshing and the doping profile of various layers of the proposed solar cell are illustrated in Fig.3 and Fig.4. The meshing parameter plays an essential role in obtaining accurate and good simulation results. According to Fig.4, to achieve accurate results, the more excellent meshing is considered at the junctions. Another critical parameter affecting the efficiency of solar cells is the photogeneration rate. The photogeneration rate gives the number of electrons generated at each point in the device due to the absorption of photons. Photo Generation is an essential parameter in solar cell operation.
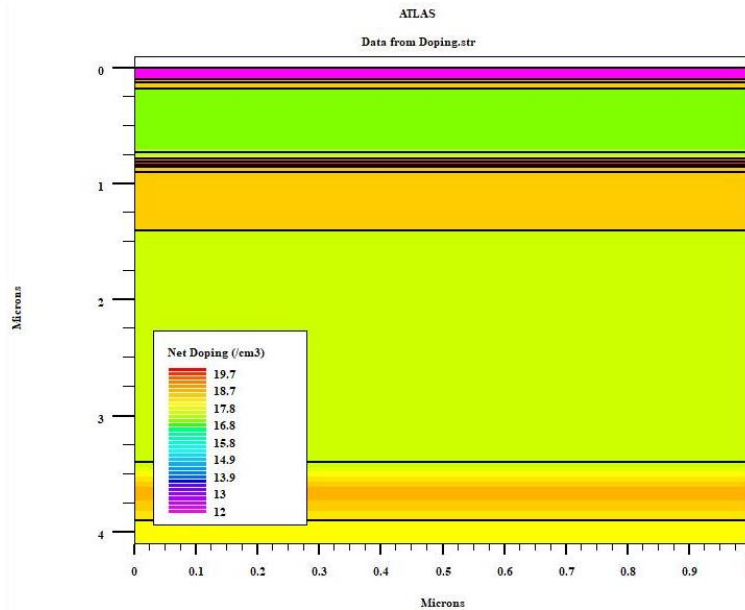
Fig.4. The doping profile of the model.

4. RESULTS AND DISCUSSION

4.1. Performance Parameters of Solar cells

A solar cell is a sandwich of n-type silicon and p-type silicon. It generates electricity by using sunlight to make electrons movement across the junction between the different layers of silicon. When sunlight shines on the cell, photons irradiate on the upper surface, photons carry their energy down through the cell, then the photons give up their energy to electrons in the lower p-type layer and elecrons use the energy to jump across the barrier into the upper, n-type layer and escape out into the circuit and the result of this process is electrons make the lamp light up. One of the important parameters of solar cell is Fill Factor, which that essentially for measurement of solar cell's quality. Fill Factor is calculated by comparing the maximum power to the theoretical power that would be output at both the open circuit voltage and short circuit current together. The FF is defined as the ratio of the maximum power from the solar cell to the product of Voc and Isc.

4.1.1. Short-Circuit Current (I_{SC}) and Open circuit voltage (V_{OC}) and Quantum Energy Gap

The short circuit current of a solar cell is the maximum current of the solar under conditions of a zero resistance load; a free flow or zero volt potential drop across the cell. The photogeneration, or the photocurrent, is another important parameter, which is a process where mobile electrons and holes are created due to the absorption of electromagnetic radiation in the semiconductor. The photogeneration rate is determined by the number of photons that generates excited electrons. The photo-generation of the presented solar cell is illustrated in Fig.5. According to Fig.5, one can see that the maximum photo-generation rate is reached at the surface and decreases as we move down the surface. Because the top cell receives maximum solar radiation, the highest photo-generation rate is achieved at the top cell. The Potential Distribution in different parts of the presented solar cell is illustrated in Fig.7.

Table 1- Material parameters used in the simulation.

| Layer properties	InGaP	AlInGaP	GaAs	CuGaSe	CNT
Layer band gap E_g(eV)	1.90	2.30	1.42	1.011	0.026
Electron affinity X_e (eV)	4.16	4.06	4.07	3.89	5.80
Relative permittivity ε_r (F cm−1)	11.62	11.70	13.50	13.60	5.40
Electron mobility μn (cm²/V s)	1945	1945	8800	100	8138.02
Hole mobility μ_p (cm²/V s)	141	141	400	25	8138.02
Conduction band effective density of states Nc (cm^{-3})	1.30×10^{20}	1.30×10^{20}	4.70×10^{19}	2.20×10^{18}	3×10^{17}
Valence band effective density of states Nv (cm^{-3})	1.28×10^{19}	1.28×10^{19}	7×10^{18}	1.80×10^{19}	3×10^{17}
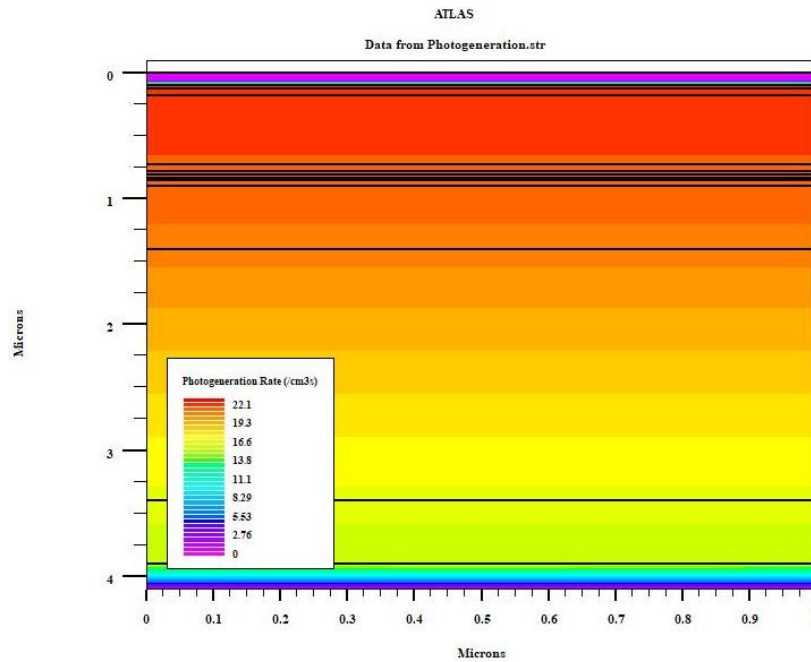
Fig.5. The photo-generation rate of the model.
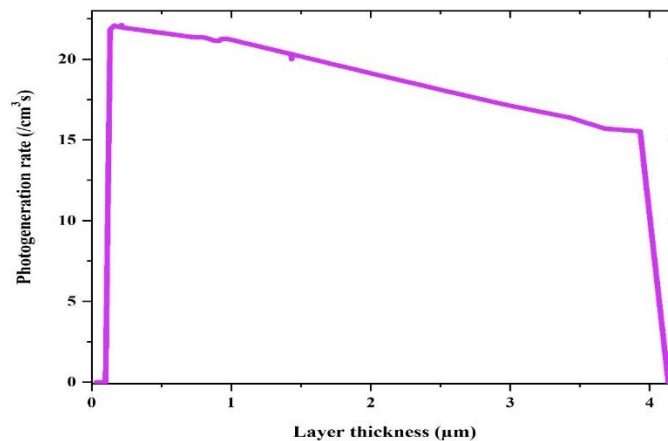
Fig. 6. Cutline view of photogeneration rate of the proposed model

The absorption of photons and the electron-hole pair (EHP) photogeneration happens mostly inside the depletion region, W, and the p-side. That charges the n-side negatively, creating an open circuit between the two regions. Not every EHP photogeneration contributes to the photovoltaic effect, but only those created in the minority carrier, diffusion length L_e, where:

$$L_e = \sqrt{2D_e \tau_e} \tag{1}$$

and D_e is the diffusion coefficient, and τ_e is the recombination lifetime.

The remaining photo-generated EHPs are lost in recombination. This is the reason that at the bottom of the cell, the p-type semiconductor is chosen, where electrons are the minority carriers. The current collected at the electrodes is called photocurrent. This current does not depend on the voltage of this junction, as there are always some. The voltage is the product of the photocurrent. Moreover, there is diode current I_d, so the total current is given by the equation:

$$I = -I_{ph} + I_0 \left(e^{\frac{eV}{nkT}} - 1 \right) \tag{2}$$

where,

$$I_d = I_0 \left(e^{\frac{eV}{nkT}} - 1 \right) \tag{3}$$

The short circuit current was given by:

$$I_{SC} = I + I_d \tag{4}$$

By setting I = 0, which means that no current flows, it is exactly the open-circuit case. The open-circuit voltage (V_{OC}) can be given as follow

$$V_{OC} = \frac{K_B T}{q} L_n \left(\frac{I_{SC}}{I_0} + 1 \right) \tag{5}$$

The equation of a quantum-energy gap is a function of how thick is well:

$$E_{QW} = E_g + \frac{\hbar^2 \pi^2}{2 m_e L^2} + \frac{\hbar^2 \pi^2}{2 m_h L^2} \tag{6}$$
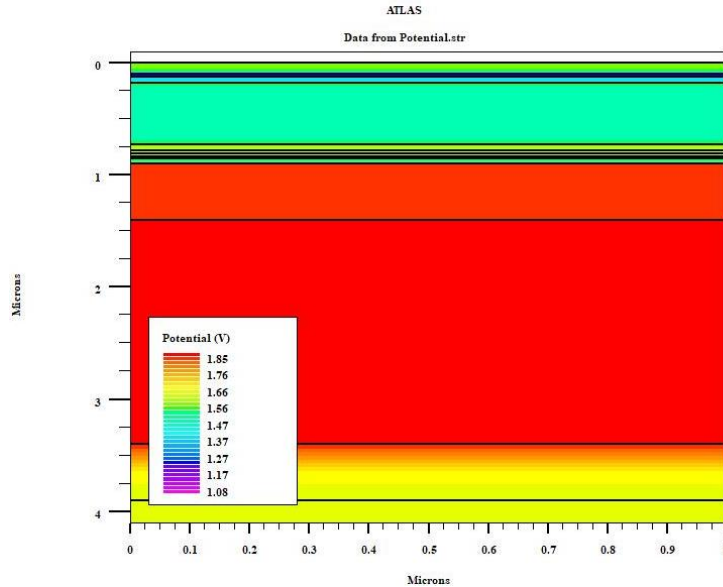

Fig.7.Potential Distribution in different parts of this model.

4.1.2 Fill factor (FF) and Efficiency (η)

In general, the power delivered from a power source can be P = IV. If we use the current density I instead, we get the power density (P_d = IV). The maximum power density occurs somewhere between V=0 (short circuit) and V=V_{oc} (open circuit) at a voltage V_m. The corresponding current density is called I_m, and thus the maximum power density is $P_m = I_m V_m$. The efficiency of a solar cell is defined as follows [11]:

$$\eta\% = \frac{P_m[W] \times 100}{1000[W.m^{-2}] \times CellArea[m^2]} \tag{7}$$

Where Pin=1000[W.m^{-2}] is the power density of the incoming light. The fill factor, FF, is another quantity used to characterize a solar cell. The fill factor can be defined as:

$$FF = \frac{I_m V_m}{I_{SC} V_{OC}} \tag{8}$$

The fill factor gives a measure of how much of the open-circuit voltage and short circuit current are utilized at maximum power. Using FF, we can express the efficiency as:

$$\eta\% = \frac{I_{OC} \times V_{OC} \times FF \times 100}{1000[W.m^{-2}] \times CellArea[m^2]} \tag{9}$$

The overall Current-voltage curve of the modified double junction InGaP/GaAs solar cells by multi-quantum well is illustrated in Fig.8. The I-V (current-voltage) curve of a PV string (or module) describes its energy since double junction solar cells consist of a series connected double stack junction solar cell with hetero tunnel junction modified by multi-quantum well, where, J_m= 35.70 [mA/cm^2] and V_m=1.49(V). In table.2, the influence of variation of the thickness of Quantum well effects on efficiency is compared, and the result has been illustrated in Fig.9. For more convincing, the important output results of the presented double junction InGaP/GaAs are compared with the previous works in Table.3. The AM1.5G spectrum, used to illuminate the proposed model, is illustrated in Fig.10.

Table 2- Different solar cell parameters with various thickness of quantum well layer For one sun.

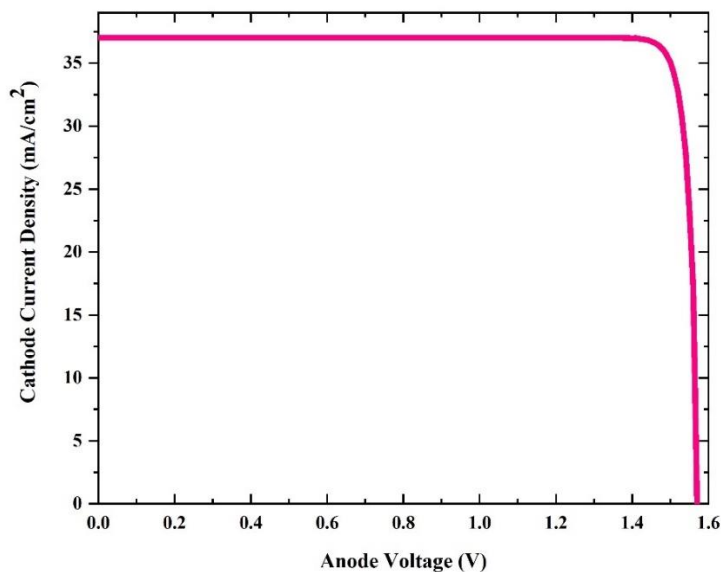| thickness (nm)	V_{OC} (V)	J_{SC} (mA/cm^2)	FF (percent)	µ(percent)
2	1.57	37.02	85.52	49.71
3	1.57	35.36	82.30	45.69
4	1.57	35.36	82.30	45.69
5	1.57	35.36	82.30	45.69

Fig.8.The overall Current-voltage curve of the modified solar cell.

Table 3- Comparison of the performance of the proposed model with the different optimized InGaP/GaAs Double Junction solar cell structures for spectrum AM 1.5G.

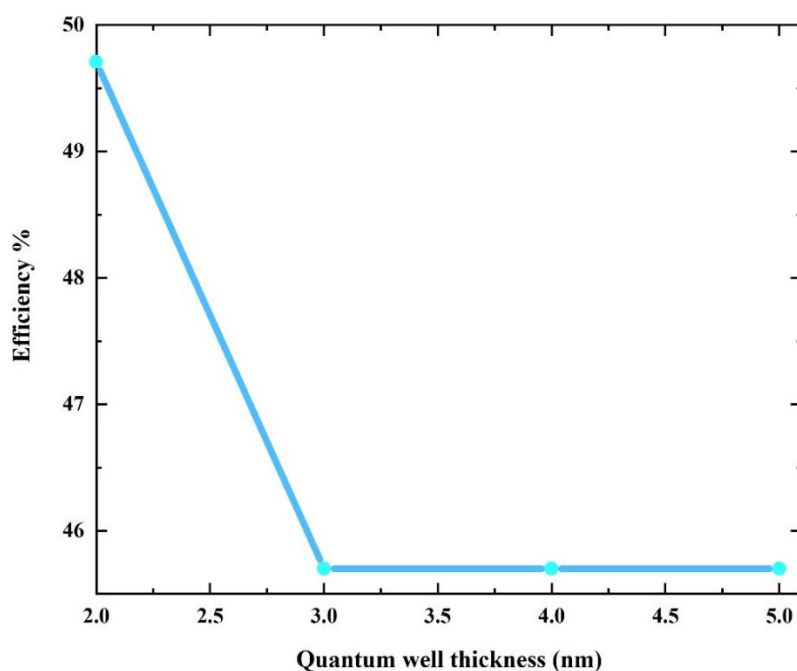| Solar Cell	V_{OC} (V)	J_{SC} (mA/cm^2)	FF (percent)	μ(percent)
Ref. [12] (Lueck et al.)	2.33	10.90	79.00	23.60
Ref. [13] (J. W. Leem et al.)	2.30	10.60	87.55	25.14
Ref.[15](F. Djaafar et al.)	2.53	15.19	91.32	25.43
Ref. [14] (K. J. Singh and S. K. Sarkar)	2.66	16.09	89.50	36.678
Ref. [6](P.P. Nayak et al.)	2.66	17.33	88.67	39.15
Ref. [7](J.P. Dutta et al.)	2.668	18.23	88.29	40.879
Ref.[1](B.Farhadi et al.)	1.75	33.23	72.20	41.95
Ref.[16](G.S.Sahoo et al.)	2.704	18.98	88.88	43.603
Ref. [17](Sh. Bagheri et al.)	2.45	17.41	88.70	36.24
Ref. [18](Chee et al.)	2.44	20.71	88.60	32.40
This work	1.57	37.02	85.52	49.71

Fig.9. Different solar cell Efficiency with various thickness of the quantum well layer

5. SUMMARY

The mean optimization of this work is the improvement of solar cell efficiency is the use of multi-quantum well in Double Junction InGaP/GaAs Solar Cell With hetero tunnel junction using a thin carbon nano Tube Layer solar cell. Quantum wells in solar cells confine electrons and holes that normally move in three dimensions to two dimensions. The number of the confined electrons and holes is determined by the thickness of the semiconductor used, usually ranging from 1-10 nanometers. Confining electrons within quantum wells allows them to be easily converted to useful forms of energy, and it is the thinness of the semiconductor material that allows this to happen. In this paper, the structure and performance of Double Junction solar cells based on InGa /GaAs were reviewed and modified by adding GaAs and CuGaSe with a thickness of 2 nm as multi-quantum well Layers. The simulation predicted that using multi-quantum wells at the top cell and bottom cell and modifying the bottom base layer thickness means the increase of the efficiency. It has been shown that for the optimized cell, the V_{OC}, J_{SC}, FF, and efficiency are 1.57 V, 37.20 [mA/cm^2], 85.52%, and 49.71%, respectively.

REFERENCES

[1] B.Farhadi, M.Naseri, A Novel Efficient Double Junction InGaP/GaAs Solar Cell Using a Thin Carbon Nano Tube Layer, Optik – Int,6224-6231,(2016).

[2] P.L.McEuen, M.Fuhrer, H.Park, Single-Walled Carbon Nanotube Electronics, IEEE, Nanotechnology, Vol. 1. No.1 (2002).

[3] L.Ji Ung, Photovoltaic effect in ideal carbon nanotube diodes, Phy's journal, Lett. 87 (3), Appl073101, (2003).

[4] G. Xiao, Y. Tao, J. Lu.Z. Zhang, Highly transparent, and conductive carbon nanotube coatings deposited on flexible polymer substrate by solution method, Proc. 3rd International Nanoelectronics Conference (INEC), pp.208–209, 3–8 ,(2010).

[5] R.R. King, N.H. Karam, J.H. Ermer, N. Haddad. Next-generation, high-efficiency III-V multi-junction solar cells, IEEE Photovoltaic Specialists Conference, p. 998, (2000).

[6] P.P. Nayak, J.P. Dutta, Efficient InGaP/GaAs DJ solar cell with double back surface field layer. Engineering Science and Technology, an International Journal, 18-325e335, (2015).

[7] J.P. Dutta, et al., Design and evaluation of ARC less InGaP/GaAs DJ solar cell with InGaP tunnel junction and optimized double top BSF layer, Optik – Int, J. Light Electron Opt,(2016).

[8] Z.Xin-He, L.San-Jie, GaInP/GaAs tandem solar cells with highly Te- and Mg-doped GaAs tunnel junctions grown by MBE, Chinese Physics B, 24(10): 108802,(2015).

[9] X.Sheng,w.C.J. Corcoran, Enhanced ultraviolet responses in thin-film InGaP solar cells by down-shifting, Phys. Chem. (15)20434, (2013).

[10] K.Tanabe, A Review of Ultrahigh Efficiency III-V Semiconductor Compound Solar Cells: Multijunction Tandem, Lower Dimensional, Photonic Up/Down Conversion, and Plasmonic Nanometallic Structures. Institute of Industrial Science, University of Tokyo, Tokyo 153–8505, (2009).

[11] T.Saga, Advances in crystalline silicon solar cell technology for industrial mass production, NPG Asia Materials, 96–102 (2010).

[12] M.R. Lueck, C.L. Andre, A.J. Pitera, M.L. Lee, E.A. Fitzgerald, S.A. Ringel, Dual junction GaInP/GaAs solar cells grown on metamorphic SiGe/Si substrates with high open-circuit voltage, IEEE Electron. Device Lett. 27-142 (2006).

[13] J.W. Leem, Y.T. Lee, J.S. Yu, Optimum design of InGaP/GaAs dual-junction solar cells with different tunnel diodes, Opt. Quantum Electron 41-605,(2010).

[14] K. Jolson Singh, S.K. Sarkar, Highly efficient ARC less InGaP/GaAs DJ solar cell numerical modeling using optimized InAlGaP BSF layers, Opt. Quant. Electron,43-1,(2012).

[15] F. Djaafar, B. Hadri, G. Bachir, Optimal parameters for performant heterojunction InGaP/GaAs solar cell, Hydrogen energy,(2016).

[16] G.S. Sahoo, P.P. Nayak, An ARC less InGaP/GaAs DJ solar cell with hetero tunnel junction, Superlattices, and Microstructures, (201

[17] Sh. Bagheri, R. Talebzadeh, B. Sardari, F. Mehdizadeh, Design and simulation of a high efficiency InGaP/GaAs multi junction solar cell with AlGaAs tunnel junction, Optik – Int, 163315, (2019).

[18] K. W.A.Chee,Y.Hu, Design and optimization of ARC less InGaP/GaAs single-/multi-junction solar cells with tunnel junction and back surface field layers, 25-39, (2018).